Deformation Morphology of Polyester Single Crystals

SURESH R. SHRAWAGI and EDWIN L. THOMAS, *Department of Chemical Engineering and Materials Science, University of Minnesota, Minneapolis, Minnesota 55455*
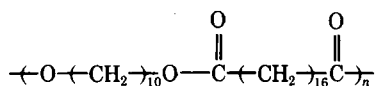
Synopsis

Truncated, six-sided single crystals of a 10–16 linear polyester were grown from dilute solution in hexanol, deposited onto Mylar film, and uniaxially deformed at room temperature. For elongations below 10%, the crystals deform uniformly; however, above 20% elongation many cracks spanned by fibrils of 300 Å diameter develop approximately normal to the applied stress direction. Depending on the position of the crystal relative to the draw direction, lateral buckling pleats and cleavage cracks can also occur. Collapse of the nonplanar crystals onto the substrate with a resulting nonuniform adherence of the crystal influences the deformation. The deformation morphology is compared to that of truncated sixfold sector polyethylene crystals. Most notably, in contrast to polyethylene, {010} fold sectors do not deform differently from {110} fold sectors and phase boundaries between {110} and {010} fold sectors do not fracture easily.

INTRODUCTION

The nature of the plastic deformation of polymer single crystals has received increasing attention during the last several years. The great majority of these investigations have been on polyethylene but all polymer single crystals thus studied deform primarily by the formation of micronecks (cracks normal to the applied stress direction, spanned by fibrils).[1] In addition to micronecking, uniform deformation,[2] crystallographic twinning,[2,3] martensitic transformation,[4] cleavage between fold planes[5] and lateral buckling[6–8] occur to various degrees depending on the particular polymer, the orientation of the crystal to the stretch direction and the total amount of deformation.

The present study concerns the deformation behavior of a 10–16 linear aliphatic polyester, poly (decamethylene 1,16-hexadecanedicarboxylate)

$$\text{+O+CH}_2\text{+}_{10}\text{O}-\overset{\displaystyle O}{\overset{\displaystyle \|}{C}}\text{+CH}_2\text{+}_{16}\overset{\displaystyle O}{\overset{\displaystyle \|}{C}}\text{+}_n$$

which crystallizes with molecular packing closely resembling truncated, six-fold sector, polyethylene single crystals. The deformation behavior of the two polymers are compared on the basis of differences in chemical structure, crystal structure, and fold plane orientation.
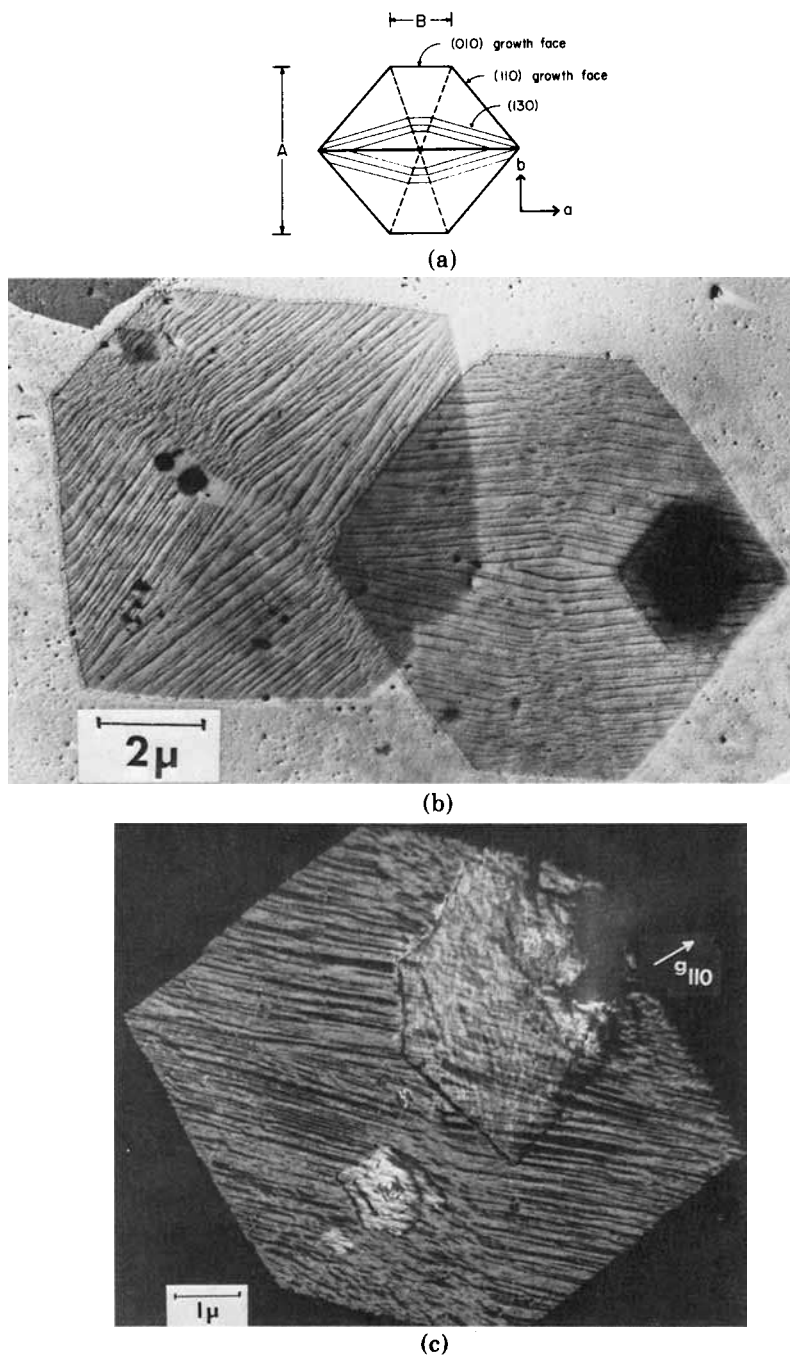
(a)

(b)

(c)

Fig. 1. (a) Schematic of a 10–16 linear polyester single crystal showing {110} and {010} fold sectors. Collapse of the nonplanar crystals upon evaporation of the solvent results in {130} and {010} collapse striations. The heavy dark line indicates (110):(1̄10) fold domain boundaries and the dotted lines indicate the {110}:{010} phase domain boundaries. (b) Bright field micrograph of undeformed 10–16 linear polyester single crystals. Notice the {130} type collapse striations in {110} sectors and {010} type collapse striations in the {010} sectors. (c) 110 dark field micrograph of undeformed crystal showing extinction bands due to molecular tilt from collapse of the nonplanar crystal onto the substrate.

EXPERIMENTAL

The polymer used in this study is the same polymer used by Kanamoto et al. in their morphology studies.[9,10] The single crystals were obtained by slowly cooling a 0.03 wt-% solution of the polyester in n-hexanol from 72°C to room temperature. The crystals are pseudohexagonal in shape and approximately 120 Å thick.

The crystals were deposited on Mylar film and uniaxially deformed various amounts at room temperature. The percent deformation cited is the average value for the Mylar only. It should be noted that the Mylar film deforms somewhat inhomogeneously so that one can only determine the approximate degree of deformation for any particular crystal.

The method of Geil[11] using polyacrylic acid for stripping the crystals from Mylar and a polystyrene coating to prevent breakup of the replica was employed. The specimens were Au–Pt shadowed at the angle $\tan^{-1}$ 1/14. The direction of shadowing was in all cases normal to the direction of drawing. The crystals were viewed at 50 KeV in an RCA EMU-4C electron microscope.

RESULTS

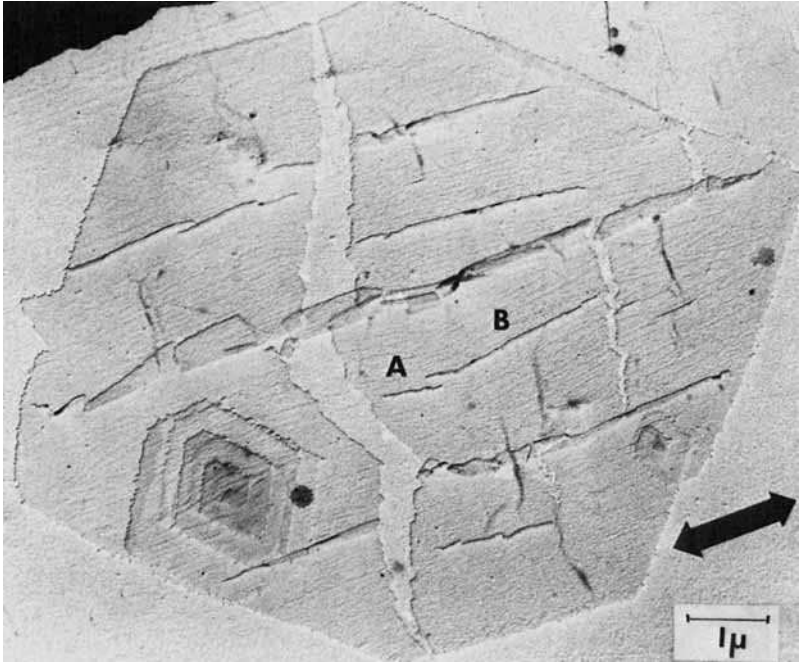### Undeformed Crystal Morphology

The polyester crystals obtained by dilute solution crystallization are shown in Figure 1. The fold planes are thought to be the growth face planes, {110} and {010}.[9] The crystals form as true lozenges at lower crystallization temperatures and true hexagons at the highest crystallization temperatures.[9] This is the same behavior noted for polyethylene.[12] The unit cell is monoclinic with a = 5.47 Å, b = 7.38 Å, c = 37 Å, β = 115°, and $a \sin \beta$ = 4.96 Å. Thus the molecular packing normal to the chain axis is almost identical to that of polyethylene.*

When the crystals are deposited onto a substrate, collapse striations form along ⟨310⟩ directions in {110} sectors and along ⟨100⟩ directions in {010} sectors. The corresponding striations observed in polyethylene are along ⟨130⟩ and ⟨010⟩ directions.[5] The presence of striations in bright field and extinction bands in dark field micrographs (see Fig. 1) indicates the crystals are nonplanar. The striations tend to disappear with time after deposition (again similar to polyethylene[13]) suggesting that slip can readily occur along the chain axis direction.
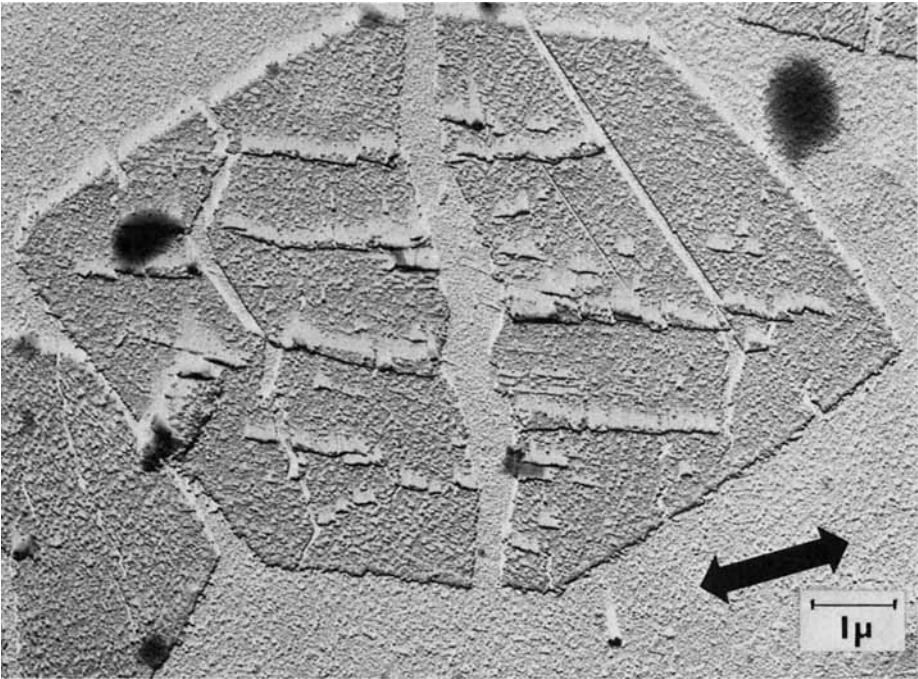
Deformation Morphology

For elongations below 10%, the crystals deform uniformly without the formation of any cracks. At extensions greater than about 20% micronecks develop approximately normal to the applied stress direction. The deformation morphology observed at these higher elongations depends markedly on the orientation of the crystal relative to the draw direction.

---

*The magnitudes of the a and b axes are just reversed for the two polymers. Hence the ($hk0$) plane or [$hk0$] direction in the polyester corresponds to the ($kh0$) plane or [$kh0$] direction in polyethylene.
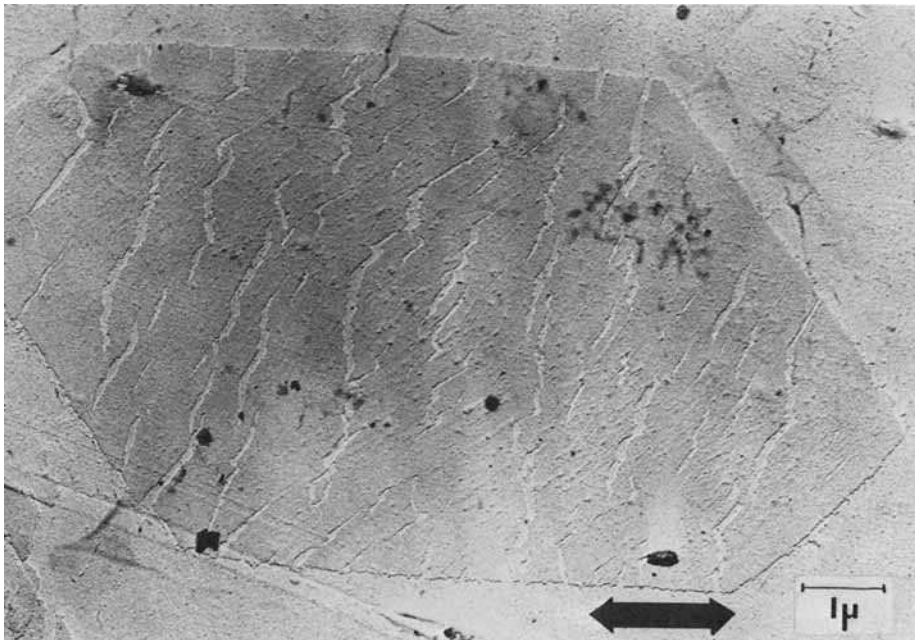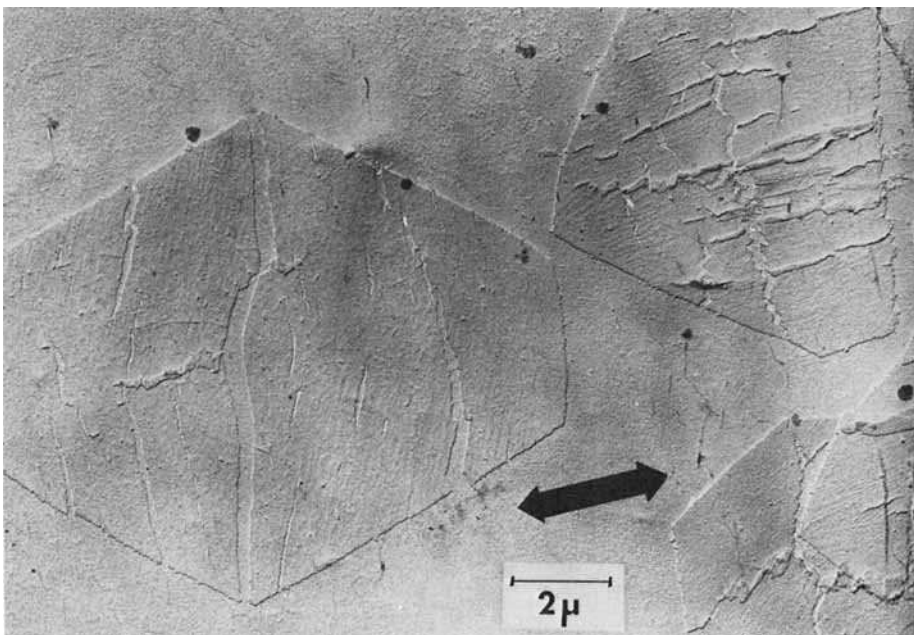
(a)

(b)

Fig. 2. (a) Bright field micrograph of a crystal deformed 30% along the a axis. Compression pleats change from [100] in the (0$\bar{1}$0) fold domain (region A) to [310] in the (1$\bar{1}$0) fold domain (region B). Direction of the applied stress is indicated by arrow on all micrographs. (b) Bright field micrograph of a crystal drawn 40% at a small angle to the a axis. {110} cleavage cracks are visible in the (110) and ($\bar{1}\bar{1}$0) fold domains.
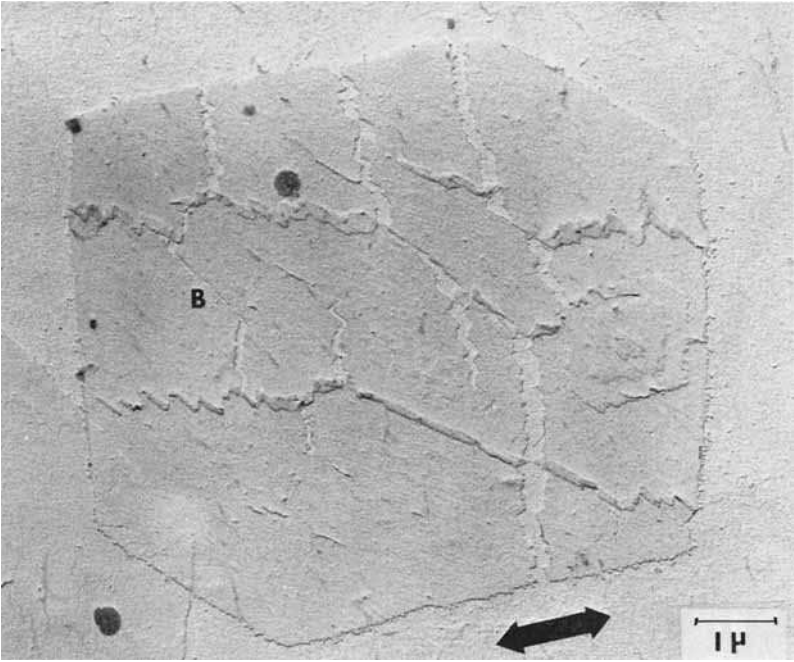
(a)

(b)

Fig. 3. (a) Bright field micrograph of a crystal deformed 40% at a small angle to the *b* axis. It is evident from the distortion of overall crystal shape that significant uniform deformation has accompanied the formation of a large number of small cracks along the ⟨310⟩ and ⟨100⟩ directions. (b) Bright field micrograph of crystals deformed 40%. The crystal on the left is *b* axis oriented while the crystal on the right is *a* axis oriented. Note the small cracks along the ⟨310⟩ and ⟨100⟩ directions and almost total absence of compression pleats for the *b* axis oriented crystal. The *a* axis oriented crystal contains a few large jagged cracks and many compression pleats along the stress direction.

(a)

(b)

Fig. 4. (a) Bright field micrograph of a crystal deformed 40% at an angle of about 45° to the a and b axes. The edges of the jagged crack and compression pleat tend to be parallel to the {010} and {110} planes. The small, short, straight compression pleats are parallel to $\langle 310 \rangle$ and $\langle 100 \rangle$. (b) Bright field micrograph of crystal drawn 40% at an angle of about 40° to the a axis. 300 Å diameter microfibrils are drawn across the large crack.

Draw along the *a* Axis

Figures 2a and 2b show several crystals drawn approximately parallel to the *a* axis. Several jagged cracks oriented approximately normal to the draw direction and spanned by drawn fibrils are evident in each crystal. Compression pleats (consisting of double thickness of lamallae from fracture and subsequent slip of one portion of the crystal over the other) lie nearly parallel to the draw direction. Such pleats form due to the difference in lateral contraction of the Mylar and the polyester. The pleats tend to form predominantly by fracture of {010} and {130} planes (see regions A and B in Figure 2a). Cleavage fracture sometimes occurs between {110} fold planes (see Figure 2b). Since the crystal shape and thickness are essentially unchanged for draw along the *a* axis up to 40%, little uniform deformation has taken place.

Draw along the *b* Axis

For crystals drawn nearly parallel to the *b* axis many small short cracks occur approximately normal to the applied stress direction. The cracks tend to occur between {130} planes in {110} fold sectors and between {010} planes in {010} fold sectors (see Figures 3a and 3b). Relatively few fibrils are drawn across cracks between {130} planes in {110} sectors and between {010} planes in {010} fold sectors.

The number of compression pleats formed for *b* axis draw is much less than for *a* axis draw (compare the crystals in Figure 3b). Crystals drawn parallel to the *b* axis become thin with the growth face angles severely distorted, indicating considerable uniform deformation has occurred in addition to microneck formation.

Draw 45° to the *a* and *b* Axes

Drawing at 45° to the *a* and *b* axes results in a deformation morphology which is a combination of the behavior observed for *a* axis and *b* axis draw. Jagged, zigzag cracks spanned by fibrils occur approximately normal to the draw direction and jagged, zigzag compression pleats occur approximately parallel to the draw direction (see Figures 4a and 4b). The tensile zigzag cracks contain some straight segments indicating cleavage fracture of {110} fold planes in {110} fold sectors. As well, the fracture path sometimes runs along ⟨310⟩ directions in {110} fold sectors (see region B, Fig. 4a). The zigzag path of the compression pleats appears to be quite similar to that of the tensile cracks. Fracture occurs between {110} fold planes and {130} planes in {110} fold sectors. There is little evidence for uniform deformation for 45° drawing.

DISCUSSION

Since 10–16 polyester crystals are very similar in both unit cell and folded chain crystal morphology to truncated sixfold sector polyethylene crystals, it is informative to discuss their deformation behavior in the light of the previous results obtained with truncated polyethylene crystals.

Truncated, sixfold sector polyethylene crystals have been drawn both uni-
axially[2] and biaxially[14] and as is the case for 10–16 polyester, the deformation
morphology depends on the orientation of the a and b axes to one draw direc-
tion.   Uniaxial drawing along the a axis (corresponding to b axis in 10–16
polyester) results in uniform deformation up to extensions of 150%.   Drawing
at an angle to the a axis results in the formation of micronecks at right angles
to the draw direction.   Zigzag cracks form preferentially in {100} fold sectors
and the boundaries between {110} and {100} fold sectors fail at strains as low
as 10%.   For deformations greater than 25%, sets of striations parallel to the
a axis, believed to be due to lateral concentration accompanying the crystal
elongation, are observed.[2]

Biaxial deformation of truncated polyethylene crystals results in crack for-
mation with strains as low as 6%.   The cracks tend to form between {020}
planes and nucleate at the edges of the {110} and {100} fold sector bounda-
ries.[14]

Based on the similarity of chemical structure and crystal morphology, it is
not surprising to observe that 10–16 polyester crystals tend to draw much
more uniformly along the b axis than along the a axis.   The ability to deform
along the stress direction for b axis oriented crystals prevents the formation
of compression pleats which occur due to compression of the undeformed
crystal by the deforming Mylar substrate for a axis oriented crystals.

The increased susceptibility to crack formation of 10–16 polyester crystals
over truncated polyethylene crystals* is probably due to the nonplanar,
ridged surface of the collapsed crystals.   Nonuniform adherence to the sub-
strate along the $\langle 310 \rangle$ and $\langle 010 \rangle$ collapse striation directions would provide
localized stress concentrations for development of the observed cracks be-
tween the {130} and {010} planes in tension and for development of the ob-
served compression pleats between {130} and {010} planes in compression.

Deformation of the crystal at an angle to the b axis results in the formation
of a few large cracks with little apparent uniform deformation.   Cleavage
parallel to {110} fold planes occurs rather infrequently and only over relatively
short distances in polyethylene.   The extremely long straight cleavage frac-
ture of {110} fold planes is strong evidence for the assumed {110} folding in
10–16 polyester (see Figures 2b and 5) and is probably due to the dipole–di-
pole interaction between ester groups of neighboring chains within the fold
plane which leads to an increased anisotropy of interchain bonding.   {110}
fold plane cleavage occurs predominantly for planes which are oriented ap-
proximately 45° to the applied stress direction (planes of maximum shear
stress) for a axis draw.   Examination of {110} fold plane cleavage shows that
the two portions of the crystal have in addition to the separation in the stress
direction, a small offset parallel to the fracture boundary.   This suggests that
cleavage is occurring due to shear parallel to the fold plane as well as tension
normal to the boundary.   Cleavage fracture for b axis orientation is probably
absent because neither the critical shear nor tensile stresses in the {110} fold
planes are reached due to the lower stress necessary for uniform deformation
and microneck formation.

An interesting difference between the truncated polyethylene crystal be-
havior and the results on 10–16 polyester crystals is the relative susceptibility

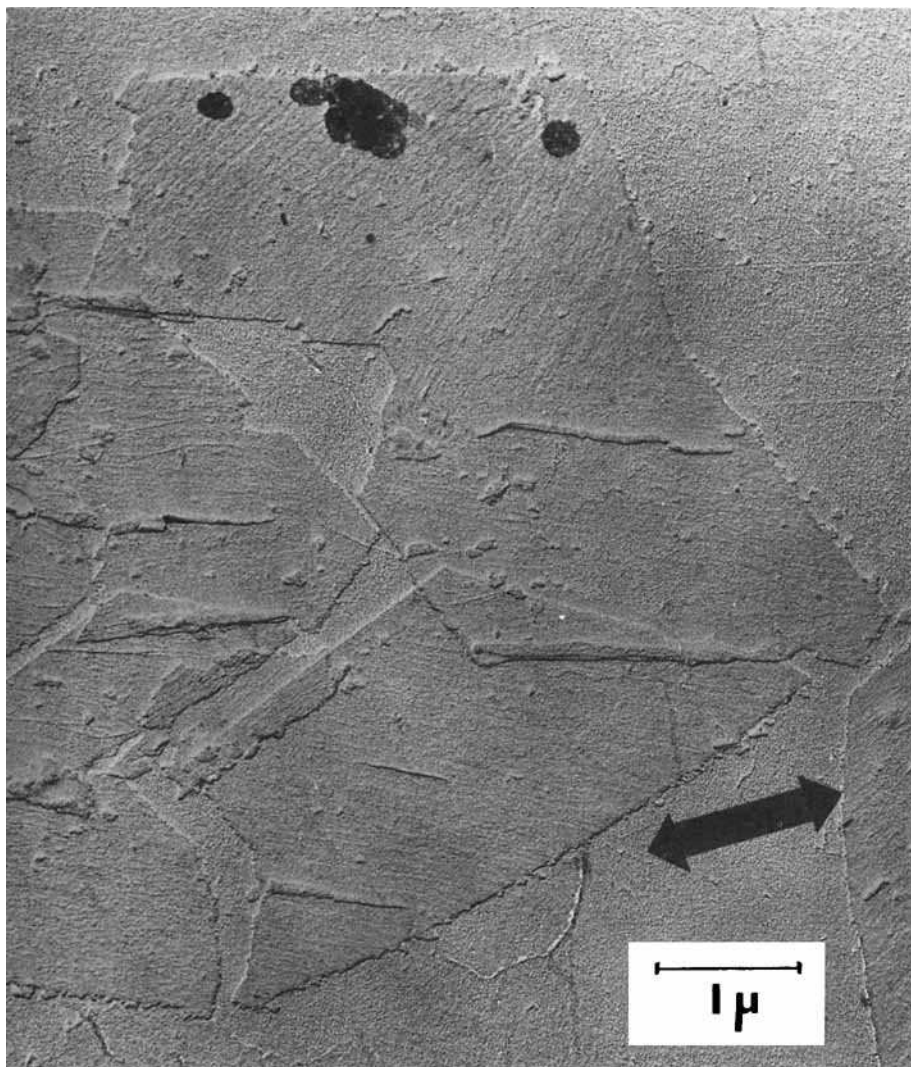*Geil's type E crystals have only one central collapse pleat.[2]

Fig. 5. Bright field micrograph of a crystal drawn 40%. The upper righthand portion of the crystal contains a growth twin boundary involving {110} fold planes. Fracture of the {010} planes resulting in ⟨100⟩ compression pleats has occurred for the portion of the twin with the *a* axis nearly parallel to the draw direction. The top portion of the twin with the *a* axis at almost 60° to the draw direction contains no compression pleats. Cleavage fracture of {110} planes is evident in both portions of the twin.

to fracture and to crack initiation of the {110}:{100} phase boundaries in polyethylene compared to the {110}:{010} phase boundaries in 10–16 polyester. Burbank has termed a phase boundary as a boundary in the crystal where both the plane of folding and the direction of folding change.[15] The geometrical requirements for smooth joining of the fold surfaces as well as fold plane continuity across the boundary require for a given fold surface plane pair (e.g., for polyethylene {110}$_{sector}$, {312}$_{surface}$, and {100}$_{sector}$, {101}$_{surface}$) a fixed A/B ratio (see Fig. 1a).[12] For other A/B ratios, the boundary contains vacancies and terminating fold planes as well as offset along the [001] direction due
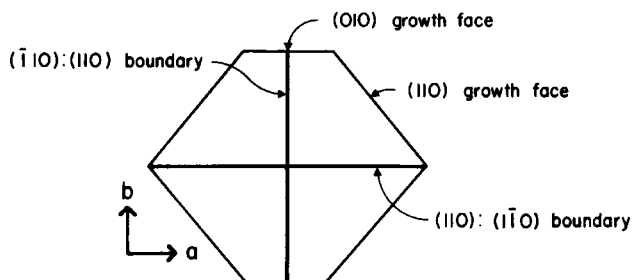
Fig. 6. Schematic of a truncated 10–16 linear polyester single crystal consisting of four {110} fold sectors.
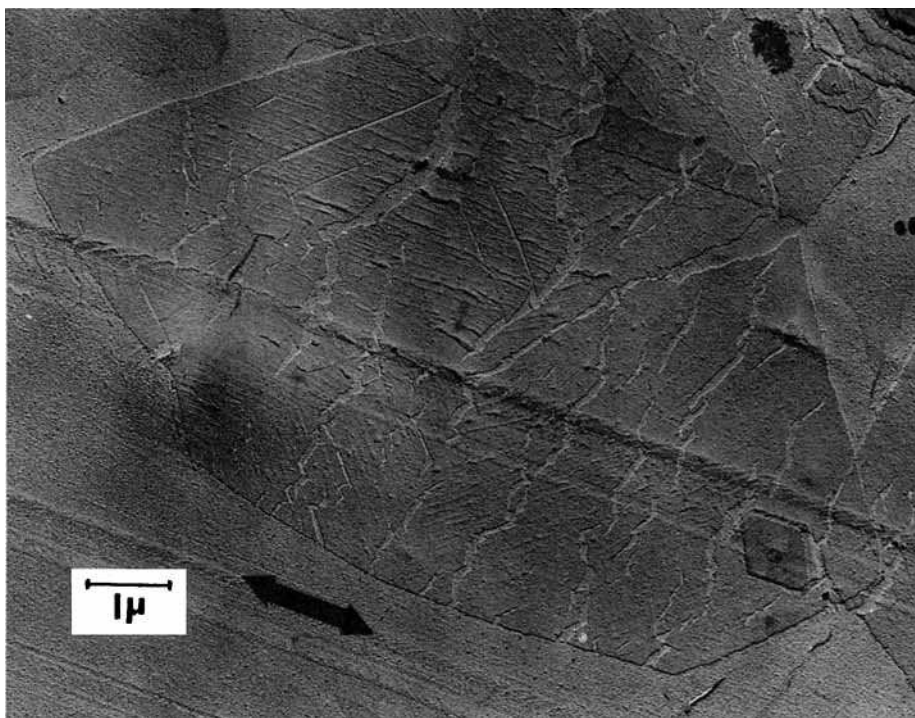

Fig. 7. Bright field micrograph of multiple twin crystal deformed approximately 30%. The lefthand portion of the crystal (a axis oriented) contains two sets of {110} cleavage cracks which intersect along a jagged crack which runs essentially parallel to the suggested ($\bar{1}10$):(110) domain boundary.

to mismatch of the respective fold surfaces.[15] These structural defects increase with deviation from the pseudohexagonal A/B ratio (the A/B ratio for the best matching is 1.5 for polyethylene). Assuming the fold surface planes in 10–16 polyester are the same as in polyethylene (not proven to date) then the polyester crystals are closer to the optimum A/B ratio than for truncated polyethylene ($A/B \simeq 4.5$ polyethylene,[2,14] $A/B \simeq 3.0$ polyester) and would therefore have stronger phase boundaries and hence fewer cracks along these boundaries.

An alternative explanation is to assume that 10–16 polyester crystals consist of only four {110} fold domains (i.e., a ($\bar{1}10$):(110) fold domain boundary

running through the center of the crystal normal to a (110):(1$\bar{1}$0) boundary) (see Fig. 6).

This type of fold domain structure eliminates the need to consider the strength of {110}:{010} phase boundaries. Such a structure also explains the unchanged character of the cleavage fracture path on crossing the (supposed) {110}:{010} phase boundaries (see Fig. 2b) and the occasional presence of two sets of {110} cleavage cracks intersecting along a jagged crack which runs parallel to the position of the suggested ($\bar{1}$10):(110) fold domain boundary (see Fig. 7). Other evidence in favor of a crystal consisting entirely of {110} folding is the lack of distinct {010} cleavage cracks. The edges of cracks formed between {010} planes are somewhat ragged and occasionally contain fibrils. Another puzzling fact is the lack of regular collapse striations along ⟨010⟩ directions in {010} fold sectors.[9] Attempts to distinguish the {110} and {010} fold sectors by melting behavior were unsuccessful, implying either a similar melting point for both sectors or the presence of only one type of fold sector.* Such a fourfold domain structure while suitably accounting for the observed deformation behavior, however, fails to explain the six-sided nature of the crystals and the collapse striation pattern. The exact nature of chain folding in these 10–16 polyester crystals therefore needs further inquiry.

*Annealing experiments have confirmed the existence of two distinct fold types in polyethylene.[16]

References

1. J. A. Sauer, G. C. Richardson, and D. R. Morrow, *J. Macromol. Sci.*, **C9**, 149 (1973).
2. P. H. Geil, *J. Polym. Sci.*, **A2**, 3813 (1964).
3. H. Kiho, A. Peterlin, and P. H. Geil, *J. Appl. Phys.*, **35**, 1599 (1964).
4. P. Allan and M. Bevis, *Phil. Mag.*, **31**, 1001 (1975).
5. D. H. Renker, *J. Polym. Sci.*, **A-3**, 1069 (1965).
6. C. A. Garber and P. H. Geil, *Makromol. Chem.*, **113**, 246 (1968).
7. P. Cerra, D. R. Morrow, and J. A. Sauer, *J. Macromol. Sci.—Phys.*, **B3** (1), 33 (1969).
8. D. R. Morrow and A. E. Woodward, *J. Macromol. Sci.—Phys.*, **B4** (1), 153 (1970).
9. T. Kanamoto, K. Tanaka, and H. Nagai, *J. Polym. Sci.*, **A2**, 2043 (1971).
10. T. Kanamoto, *J. Polym. Sci.*, **12**, 2535 (1974).
11. P. H. Geil, *Polymer Single Crystals*, Interscience, New York, 1963.
12. T. Kawai and A. Keller, *Phil. Mag.*, **11**, 1165 (1965).
13. A. Keller, *Kolloid Z. Z. Polymere*, **197**, 98 (1964).
14. K. Hass and P. H. Geil, *J. Polym. Sci.*, **A2**, 289 (1966).
15. R. D. Burbank, *Bell System Tech. J.*, **39**, 1627 (1960).
16. H. Nagai and N. Kajikawa, *Polymer*, **9**, 177 (1968).